Optimal AC/DC distribution systems expansion planning from DSO's perspective considering constraints

Heitor Farias de Barros, Marie-Cécile Alvarez-Hérault, Bertrand Raison, Quoc Tuan Tran

Optimal AC/DC Distribution Systems Expansion Planning From DSO's Perspective Considering Topological Constraints

Heitor Farias de Barros, *Student Member, IEEE*, Marie-Cécile Alvarez-Herault, *Member, IEEE*, Bertrand Raison, *Senior Member, IEEE*, and Quoc Tuan Tran, *Senior Member, IEEE*

***Abstract*—As the integration of DC distributed resources increases in recent years, hybrid AC/DC topology emerges as a promising alternative in the planning of distribution systems. This article presents an AC/DC optimal expansion planning of distribution networks from Distribution System Operator's perspective with a special focus on grid architecture through Integer Programming-based topological constraints. The proposed formulation aims to determine the optimal location and sizing of converters and to select lines type (AC or DC) and state (closed or open). The problem is formulated as a mixed integer second-order conic programming model that guarantees global optimality and verifiable exactness by using off-the-shelf solvers. A multi-scenario approach with a Wasserstein distance-based scenario reduction is applied to deal with resource uncertainty. Case studies based on a 13 bus and IEEE 33 bus distribution networks were used to verify the effectiveness of the model. The results show that a hybrid architecture can improve the efficiency of the grid through optimal active power flow and reduce the total network costs.**

***Index Terms*—AC/DC distribution systems, distribution system planning, optimal topology planning, radiality constraints, network configuration, mixed-integer second order conic programming.**

NOMENCLATURE

Sets

$\mathcal{N}$	Set of nodes of distribution network.
$\mathcal{N}_{\mathcal{S}}$	Set of HV/MV AC substation nodes.
$\mathcal{N}_{\mathcal{NS}}$	Set of nodes except HV/MV AC substation nodes, i. e. $\mathcal{N} \setminus \mathcal{N}_S$.
$\mathcal{N}(ij)$	Set of nodes connected by line ij, i. e. nodes i and j.
$\mathcal{L}$	Set of directed lines/branches oriented from i to j.
$\mathcal{L}_{in}(i)$	Set of lines for which i is the child node.
$\mathcal{L}_{out}(i)$	Set of lines for which i is the parent node.
$\mathcal{L}(i)$	Set of lines connected to node i.
$\mathcal{S}$	Set of scenarios.
$\mathcal{T}$	Set of years of planning study.

Indices

$\diamond_i, \diamond_j$	Index for nodes.
$\diamond_{ij}$	Index for lines.
$\diamond^s$	Index for scenarios.
$\diamond^k$	Index for fictitious commodity.
$\diamond_t$	Index for time in years.

Binary variables

α_i	AC node state (1 if there is an AC line connected to node i, 0 otherwise).
β_i	DC node state (1 if there is a DC line connected to node i, 0 otherwise).
δ_{ij}	AC/DC line state (1 if line ij is AC, 0 if DC).
γ_{ij}	Line state (1 if line ij is closed, 0 if open).
ϵ_{ij}	AC spanning tree line state (1 if line ij belongs to AC spanning tree, 0 otherwise).
λ_{ij}	DC spanning tree line state (1 if line ij belongs to DC spanning tree, 0 otherwise).
θ_{ij}	AC closed line state (1 if line ij is AC and closed, 0 otherwise).
ζ_i	Voltage Source Converter (VSC) node state for line conversion into DC (1 if there is a converter at node i, 0 otherwise).

Continuous variables

$v^s_{ac,i}$, $v^s_{dc,i}$	AC and DC squared voltage at node i in scenario s in pu.
$P^s_{ac,i}$, $P^s_{dc,i}$	AC and DC net active power injection at node i in scenario s in pu.
$Q^s_{ac,i}$	AC net reactive power injection at node i in scenario s in pu.
$P^s_{g,ac,i}$, $Q^s_{g,ac,i}$	Active and reactive power injection of AC dispatchable distributed generation at node i in scenario s in pu.
$Q^s_{g,dc,i}$	Reactive power injection of DC distributed generation through local converter at node i in scenario s in pu.
$p^s_{ac,ij}$, $p^s_{dc,ij}$	AC and DC active power in line ij in scenario s in pu.

$q^s_{ac,ij}$	AC reactive power in line ij in scenario s in pu.
$l^s_{ac,ij}$, $l^s_{dc,ij}$	AC and DC squared current in line ij in scenario s in pu.
$P^s_{vsc,ac,i}$	VSC active power injection at node i on AC side in scenario s in pu.
$P^s_{vsc,dc,i}$	VSC active power injection at node i on DC side in scenario s in pu.
$Q^s_{vsc,ac,i}$	VSC reactive power injection at node i on AC side in scenario s in pu.
$S_{vsc,rated,i}$	VSC rated power at node i in pu.
$P^s_{vsc,l,i}$	VSC total losses at node i in scenario s in pu.
$P^s_{vsc,l0,i}$	VSC losses term proportional to its rated apparent power at node i in scenario s in pu.
$P^s_{vsc,l1,i}$	VSC losses term proportional to its operating apparent power at node i in scenario s in pu.
$f^k_{ac,ij}$, $f^k_{dc,ij}$	AC and DC flow of fictitious commodity in line ij.
$CAPEX$	Capital Expenditures in \$.
$OPEX$	Operational Expenditures in \$.
OC_{vsc}	VSC operational and maintenance cost in \$.
L_{vsc}	Weighted average of VSC losses in all the scenarios in pu per year.
L_{lines}	Weighted average of lines losses in all the scenarios in pu per year.
Binary parameters	
a_i	AC node resource state (1 if there is an AC load or generation at node i, 0 otherwise).
Continuous parameters	
$P^s_{g,dc,i}$	DC active power generation at node i in scenario s in pu.
$P^s_{d,ac,i}$, $P^s_{d,dc,i}$	AC and DC active power demand at node i in scenario s in pu.
$Q^s_{d,ac,i}$	Reactive power demand at node i in scenario s in pu.
$r_{ac,ij}$, $r_{dc,ij}$	AC and DC resistance of line ij in pu.
$x_{ac,ij}$	Reactance of line ij in pu.
c_0	VSC loss coefficient proportional to its rated apparent power.
c_1	VSC loss coefficient proportional to its operating apparent power.
d	Discount rate in %.
cc_{vsc}	VSC capital cost coefficient in \$/pu.
$oc_{c,vsc}$	VSC operational and maintenance cost coefficient, as a % of capital cost.
lc	Losses cost in \$/pu.
w^s	Weight coefficient of scenario s.
$m^s_\diamond$	Power output modulation coefficient for load demand (LD), photo-voltaic (PV), wind turbine (WT) and electrical vehicle (EV) of scenario s.
$\overline{\diamond}$, $\underline{\diamond}$	Maximum and minimum limits of variable.

I. Introduction

THE high integration of DC Distributed Energy Resources (DER) is likely to cause significant changes in planning and operation of distribution systems. Indeed, networks operating fully in AC at the distribution level are prone to several problems caused by the presence of highly variable DC resources, such as voltage control issues, line overload and high losses because of excessive number of AC/DC conversion stages [1], [2], [3].

Furthermore, some AC distribution networks have ring topology at MV level, but are predominantly required to operate radially to avoid high short-circuit current and to simplify fault management. In opposition, AC/DC distribution topology have a superior meshing capacity, because DC links can be used to connect AC feeders in normal operation while AC and DC networks fault behavior can be nearly decoupled with an appropriate fault management, i.e. coordination between converter blocking capability and circuit breakers [4]. For that reason, an evolution of MV distribution networks into an AC/DC topology emerges as a promising option in Distribution System Planning (DSP) problems.

Hybrid distribution grid architecture is qualitatively discussed in [5], but AC/DC DSP mathematical formulation as an optimization problem is an ongoing subject in literature. Moreover, because of the high degree of non-linearity and discreteness, AC/DC DSP is a harder computational problem than traditional AC planning [3]. Accordingly, structural hybrid DSP, where Distribution System Operator (DSO) decides the sizing and siting of converters and feeders, is an active research topic with room for advances specially in problem formulation and solving.

Most of publications in the field of structural hybrid AC/DC DSP develops formulations to propose an optimal allocation and sizing of Voltage Source Converters (VSCs) and selection between AC and DC feeders [6], [7], [8], [9], [10], [11], [12], [13]. The Net Present Value (NPV) is typically considered as the objective function, but other operational metrics can be targeted, such as network losses and voltage deviation. The set of constraints regularly considers nonlinear power flow equations, operational limits and discrete decisions to optimally site DER and consider topological restrictions. Therefore, AC/DC DSP is frequently formulated as a Mixed Integer Nonlinear Programming (MINLP), but Mixed Integer Second Order Conic (MISOCP) relaxations and Mixed Integer Linear Programming (MILP) approximations are commonly applied to cope with intrinsic complexity of the problem and to avoid very time-consuming models.

As a matter of fact, the trade-off between optimality, exactness and computational burden is a fundamental aspect in AC/DC DSP modelling. MINLP models are usually formulated as a bi-level optimization problem and solved by meta-heuristic algorithms combined with either a numeric formulation of power flow or a nonlinear optimization solver to obtain exact results in a restrained time, but with limited guarantees of optimality [6], [7], [8], [9], [10]. In the case of MISOCP and MILP formulations, commercial off-the-shelf solvers are generally used, providing global optimality by applying Branch-and-Cut (B&C) or Branch-and-Bound (B&B) algorithms at the expense of running time [14]. Since MILP models are approximations, exactness is also disregarded. Thereupon, MISOCP relaxation for power flow constraints represents a good compromise since

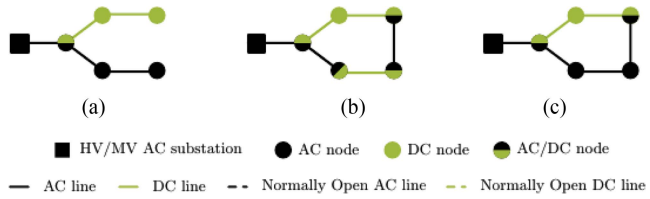

Fig. 1. Illustration of an AC/DC distribution network (a) radial, (b) meshed but piecewise radial with one AC line disconnected from substation and (c) meshed but piecewise radial, with all AC lines connected to the substation.

it has been consistently shown to be exact for AC/DC power flow applications (see [11], [12], [15], [16], [17]).

A. Topological Modeling of AC/DC DSP

The majority of AC/DC topology planning literature considers radial operation either only for the AC network or for the whole AC/DC network. The first is done by Integer Programming (IP)-based constraints in [12], i.e. expressed in a mathematical programming model, whereas the latter is done by considering inherently radial case studies in [6], [11] and [18]. [7] and [9] imposed radiality for the whole AC/DC grid through Minimum Spanning Tree (MST) algorithms and [13] did the same through IP-based constraints.

Notwithstanding, because of the AC/DC decoupling during fault and other protection reasons previously mentioned, DSO may require both AC and DC parts of the grid to be radial without imposing radiality to the whole AC/DC grid. For instance, this is a common premise in planning studies considering multiple DC links/Soft Open Points (SOP) into distribution systems [19]. In this work, this AC/DC topology is henceforth referred as piecewise radial, in opposition to (fully) radial. Fig. 1 depicts the difference between an AC/DC grid (a) radial and (b)/(c) meshed but piecewise radial.

It can also be required that AC distribution networks must be connected to the transmission system through HV/MV substation only by AC lines to ensure a simple and reliable operation. For radial networks, this is equivalent to impose that DC grid is downstream of AC grid, as proposed in [11]. For meshed grids, this requires a different set of constraints that are further developed in this article. Fig. 1 illustrates the difference between meshed AC/DC distribution system with a part of the AC lines disconnected to the HV/MV substation (b) and another with all the AC lines connected to the substation (c).

To the best of authors' knowledge, none of aforementioned AC/DC DSP formulations found in literature fully consider specific topological requirements that can be stipulated by the DSO for MV AC/DC networks here presented.

B. Cost Modeling

AC/DC DSP reviewed papers also typically consider case studies from scratch to propose a distribution system to a newly established area of load and generation (greenfield distribution planning). For this reason, DER installation, line construction and energy supply costs are considered in the planning (see [8], [10], [12]). In opposition, [6] and [13] address expansion planning, where load growth and DER connection to an existing system are considered rather from the DSO standpoint. Nevertheless, [13] predetermines AC and DC regions without evaluating the possibility of a full AC system and [6] considers the costs of converters despite of the function performed in the grid, i.e. either to simply connect a DC resource/load to the AC system (local converter) or to convert a part of the system into DC (system converter).

In practice, many electricity markets, such as the European one, are regulated under a DSO unbundling policy [20], i.e. separation of distribution system operation from other activities, such as generation. This means that the DSO does not own either DERs or related local converters, as they are installed at DER sites and are solely used by DER owners to connect their resources to the grid. In these cases, according to [21], network planning with DER can be formulated from two perspectives: the DER owners' perspective, who are interested in minimizing their own costs, and the DSOs' perspective, who are performing network planning under uncertainties caused by DER to minimize its own cost. Since topological planning is addressed in this work and DSOs are the stakeholders able to perform it, this paper focuses on expansion planning from the perspective of DSOs.

In this context, the hypotheses assumed in the literature considering local converter costs artificially increase the total planning expenditures of full AC topology. Ultimately, this promotes hybrid AC/DC architecture and limits results validity for DSOs operating under unbundling regulation aiming to study hybrid distribution system expansion. Therefore, to better model the planning problem from the point of view of network operators, DER and converter ownership aspects should be considered to obtain accurate results.

C. Contributions

The main goal of this article is to develop a distribution system expansion planning formulation that appropriately considers topological constraints, with verifiable exactness and global optimality guaranteed. In this way, the proposed formulation aims to study the benefits of changing an AC network into a hybrid topology focusing on DSO costs. Therefore, the main contributions of this work is two-fold:

- Considering topological requirements such as radiality for AC and DC parts of distribution network, but not necessarily for the whole AC/DC grid, as well as enforcing AC lines to be connected to the HV/MV susbtation. This is done through an Integer Programming-based formulation that can be incorporated to the optimization problem ensuring optimality.
- Studying the cost-effectiveness of AC/DC topology from a DSO perspective operating under unbundling regulation by proposing a hybrid expansion planning considering the difference between system converters and local converters;

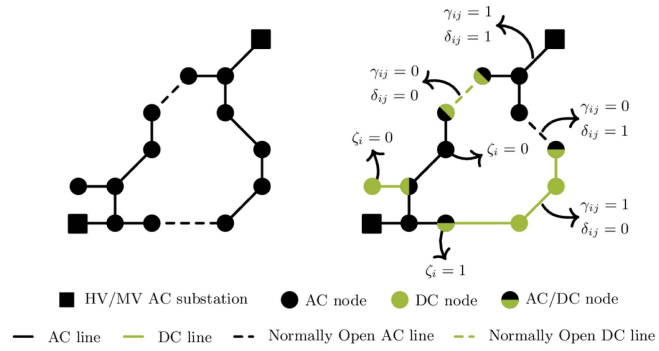

Fig. 2. Example of an AC distribution network (left) and corresponding AC/DC optimal topology planning (right) with main binary decision variables.

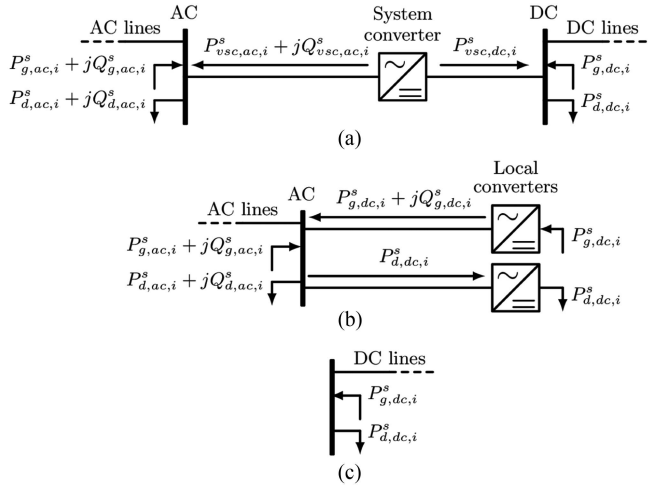

Fig. 3. Topology of (a) AC/DC node with a system converter ($\zeta=1$), pure AC node ($\alpha=1$, $\beta=0$) with only local converters ($\zeta=0$) and (c) pure DC node ($\alpha=0$, $\beta=1$).

II. Problem Description

This study aims to optimally site, size and operate multiple AC/DC converters, considering conversion of AC lines into DC and network configuration in a distribution grid. Hence, the optimal topology DSP problem consists of three main binary decisions (see Fig. 2):

1) δ: Operation of each line as either AC ($\delta=1$) or DC ($\delta=0$);
2) γ: Operation of each line as normally closed ($\gamma=1$) or normally open ($\gamma=0$);
3) ζ: To install ($\zeta=1$) or not ($\zeta=0$) a system converter at each node.

The planning is formulated to minimize the present value of the total costs over the planning horizon for a set of representative scenarios. The design of each converter rated apparent power and corresponding setting of power reference on each scenario constitute respectively the sizing and operational decisions of this planning problem. Every node and line is a candidate considered in the optimization. Thus, every node can become AC/DC or DC node and every line can be AC or DC.

The method developed here is intended to be used to propose modifications in distribution networks, in opposition to planning from scratch. In this way, distribution network is presumed to be originally operated in AC, no line construction is considered and all the system converters used to form AC/DC nodes are supposed to be installed and operated by the DSO. Local converters used to connect DC resources to pure AC nodes are supposed to be installed by the respective owners of DC resources and are not considered in DSO cost computation. AC topology is then prioritized because the system is already operated in this way and clients will not be required to adapt their voltage to be connected to the grid. Therefore, if there are AC resources in a node, it cannot be a pure DC node and a system converter needs to be installed in the substation. AC/DC, pure AC and pure DC node topology are illustrated in Fig. 3.

Voltage control is assumed to be performed by HV/MV AC substation through on-load tap changer transformer and by distributed generation through optimal reactive power support. Thereby, conventional solutions easier to implement than AC/DC topology are already considered in the DSP avoiding excessive benefits of DC architecture coming predominantly from reactive power support by the power converters. Note that only MVDC resources are addressed here, assuming that LVDC resources have a stage of conversion to step up voltage to be connected to the MVDC level which is not paid by the DSO.

III. Formulation of the Planning Model

The proposed optimal AC/DC DSP model aims to minimize objective function described in (1), detailed by (2)–(6), subject to the constraints defined by (8)–(60). The organization of this section is then as follows. First, the objective function is presented and detailed in Section III-A. Next, the constraints are presented in the following subsections. Topological constraints are described in Section III-B, power flow equations for the AC and DC networks as well as VSC constraints are presented in Section III-C. Finally, operational limits are provided in Section III-D.

A. Objective Function

In most part of literature, the DSP problem comes down to an economic optimization considering the Net Present Value. Subsequently, the objective function is formulated as in (1), minimizing the sum of Operational Expenditures (OPEX) converted into present value and Capital Expenditures (CAPEX) over a set of scenarios $\mathcal{S}$ illustrating relevant operating points. Therefore, topology is optimized with respect to these scenarios considering a weight coefficient w^s representing the probability of occurrence obtained through a scenario reduction technique discussed later.

The objective function is detailed in (2)–(6). CAPEX considers converters capital cost (see (2)), whereas OPEX contemplates converter operational and maintenance cost (OC_{vsc}), line losses (L_{lines}) and converters losses cost (L_{vsc}) (see (3)). Each of these terms is detailed in (4)–(6).

$$\min \quad CAPEX + \sum_{\mathcal{T}} \frac{1}{(1+d)^t} OPEX_t \tag{1}$$

$$CAPEX = cc_{vsc} \sum_{\mathcal{N}} S_{vsc,rated,i} \tag{2}$$

$$OPEX_t = OC_{vsc} + lc(L_{vsc} + L_{lines}) \tag{3}$$

$$OC_{vsc} = oc_{c,vsc} cc_{vsc} \sum_{\mathcal{N}} S_{vsc,rated,i} \tag{4}$$

$$L_{vsc} = 365 \times 24 \times \sum_{\mathcal{S}} w^s \sum_{\mathcal{N}} P^s_{vsc,l,i} \tag{5}$$

$$L_{lines} = 365 \times 24 \times \sum_{\mathcal{S}} w^s \sum_{\mathcal{L}} (r_{ac,ij} l^s_{ac,ij} + r_{dc,ij} l^s_{dc,ij}) \tag{6}$$

Next, in order to fully explore the technical potential of AC/DC topology, a losses minimization planning was also tested. Thus, (7) was used as objective function in this case.

$$\min \quad L_{vsc} + L_{lines} \tag{7}$$

B. Topological Constraints

- Basic topological constraints

The basic topological constraints establish the relation between binary variables and parameters concerning grid architecture ((8)–(13)). Eqs. (8)–(9) impose that if and only if an AC line is connected to node i, then, $\alpha_i = 1$. The same relation is imposed by (10)–(11) for DC lines connected to node i and β_i. Eqs. (12)–(13) impose $\zeta_i = 1$ when there are DC lines and AC lines or resources simultaneously connected to a node.

$$\delta_{ij} \leq \alpha_i \qquad \forall ij \in \mathcal{L} \quad \forall i \in \mathcal{N}(ij) \tag{8}$$

$$\alpha_i \leq \sum_{\mathcal{L}(i)} \delta_{ij} \qquad \forall i \in \mathcal{N} \tag{9}$$

$$1 - \delta_{ij} \leq \beta_i \qquad \forall ij \in \mathcal{L} \quad \forall i \in \mathcal{N}(ij) \tag{10}$$

$$\beta_i \leq \sum_{\mathcal{L}(i)} (1 - \delta_{ij}) \qquad \forall i \in \mathcal{N} \tag{11}$$

$$\alpha_i + a_i - a_i \alpha_i + \beta_i - 1 \leq \zeta_i \qquad \forall i \in \mathcal{N} \tag{12}$$

$$\zeta_i \leq (\alpha_i + a_i - a_i \alpha_i + \beta_i)/2 \qquad \forall i \in \mathcal{N} \tag{13}$$

- Piecewise radiality constraints

For protection simplicity reasons, DSOs typically operate networks radially. Although several ways to impose a radial topology using IP constraints have been carefully studied in the AC reconfiguration problem [22], [23], [24], [25], IP-based radiality and topological constraints for AC/DC network configuration have not yet been exhaustively explored in the literature.

Indeed, AC/DC distribution networks are not necessarily required to be radial, but each sub-grid (AC sub-grid or DC sub-grid) may be required to be radial. In practice, AC sub-grids are required to be radial for the same reasons mentioned for full AC distribution systems. In contrast, DC sub-grids can either be required to be radial or allowed to be meshed depending on the protection scheme, converters control and topology. In hybrid HV transmission systems, meshed Multi Terminal DC grids can be authorized because a more complex and expensive protection scheme is allowed. Up to the moment, there is no consensus whether future MVDC distribution grids will follow AC distribution radial architecture or HVDC transmission meshed architecture. In this article, a radial DC architecture is also imposed for protection aspects previously underlined.

Hence, it is assumed here that both AC and DC sub-grids are individually required to operate radially (piecewise radial), but that the union of AC and DC networks can contain loops. In other words, let $\mathcal{G}$ be the connected graph representing all lines and nodes of the network and $\mathcal{G}^{ac}$ and $\mathcal{G}^{dc}$ be the sub-graphs representing AC and DC closed lines. Then, it is assumed here that $\mathcal{G}^{ac}$ and $\mathcal{G}^{dc}$ are enforced to be forests of $\mathcal{G}$. There are no requirements, however, for the set of closed lines of the network (AC and DC), i.e. $\mathcal{G}^{ac} \cup \mathcal{G}^{dc}$ can contain loops.

In fact, [25] developed a useful formulation with compatible topological constraints for an AC microgrid formation application, where each microgrid is required to operate radially. In that case study, the set of microgrids graph can be seen as a spanning forest of $\mathcal{G}$. This is done by firstly defining a spanning tree $\mathcal{G}^{ac,st}$ of $\mathcal{G}$ by a directed multi-commodity flow formulation. Thereupon, closed lines are enforced to be a sub-graph of this spanning tree ($\mathcal{G}^{ac} \in \mathcal{G}^{ac,st}$). This is possible because a spanning forest of a connected graph is also a sub-graph of a spanning tree of the same connected graph [25].

In this article, this multi-commodity flow formulation is adapted to create respectively AC and DC graphs $\mathcal{G}^{ac,st}$ and $\mathcal{G}^{dc,st}$ that are spanning trees of $\mathcal{G}$ through the constraints depicted in (14)–(23). Eqs. (14)–(15) enforce spanning trees to have the number of branches equal to number of nodes minus the number of HV/MV substation nodes. Eqs. (16)–(17) assign one fictitious commodity k to be provided by the source node (HV/MV substation). Eqs. (18)–(19) assign one different fictitious commodity k to be consumed by each sink node (MV/LV substations) when $k = i$ and (20)–(21) enforces no commodity consumption otherwise ($k \neq i$). Then, (22)–(23) impose that fictitious commodity can only flow through branches belonging to the spanning tree.

To make each AC/DC sub-grid radial, $\mathcal{G}^{ac}$ and $\mathcal{G}^{dc}$ are respectively required to be forests of $\mathcal{G}$, i.e. sub-graphs of $\mathcal{G}^{ac,st}$ and $\mathcal{G}^{dc,st}$ (24)–(25). Finally, (26) is considered to allow loops in the whole AC/DC grid. A simple example with the graphs $\mathcal{G}$, $\mathcal{G}^{ac,st}$, $\mathcal{G}^{dc,st}$, $\mathcal{G}^{ac}$, $\mathcal{G}^{dc}$ and the union of $\mathcal{G}^{ac}$ and $\mathcal{G}^{dc}$ is shown in Fig. 4. These constrains can be easily adapted to allow loops in DC sub-grid by neglecting (15), (17), (19), (21), (23) and (25).

$$\sum_{\mathcal{L}} \epsilon_{ij} = |\mathcal{N}| - |\mathcal{N}_S| \tag{14}$$

$$\sum_{\mathcal{L}} \lambda_{ij} = |\mathcal{N}| - |\mathcal{N}_S| \tag{15}$$

$$\sum_{k \in \mathcal{N}_S} \left(\sum_{\mathcal{L}_{in}(i)} f^k_{ac,ij} - \sum_{\mathcal{L}_{out}(i)} f^k_{ac,ij} \right) = -1 \quad \forall i \in \mathcal{N}_{\mathcal{NS}} \tag{16}$$

$$\sum_{k \in \mathcal{N}_S} \left(\sum_{\mathcal{L}_{in}(i)} f^k_{dc,ij} - \sum_{\mathcal{L}_{out}(i)} f^k_{dc,ij} \right) = -1 \quad \forall i \in \mathcal{N}_{\mathcal{NS}} \tag{17}$$

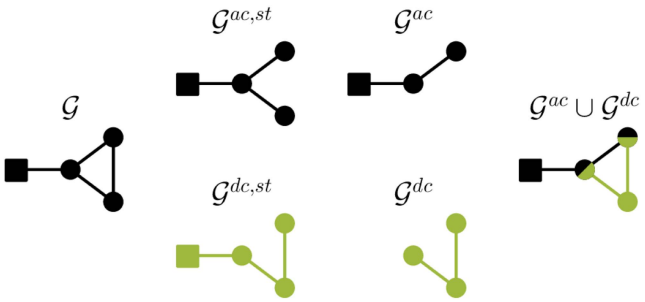

Fig. 4. Example of topological constraints applied to graph $\mathcal{G}$ and corresponding relevant sub-graphs for the formulation: $\mathcal{G}^{ac,st}$, $\mathcal{G}^{dc,st}$, $\mathcal{G}^{ac}$, $\mathcal{G}^{dc}$ and $\mathcal{G}^{ac} \cup \mathcal{G}^{dc}$.

$$\sum_{\mathcal{L}_{in}(i)} f^k_{ac,ij} - \sum_{\mathcal{L}_{out}(i)} f^k_{ac,ij} = 1 \quad \forall i \in \mathcal{N}_{\mathcal{NS}} \quad \forall k = i \tag{18}$$

$$\sum_{\mathcal{L}_{in}(i)} f^k_{dc,ij} - \sum_{\mathcal{L}_{out}(i)} f^k_{dc,ij} = 1 \quad \forall i \in \mathcal{N}_{\mathcal{NS}} \quad \forall k = i \tag{19}$$

$$\sum_{\mathcal{L}_{in}(i)} f^k_{ac,ij} - \sum_{\mathcal{L}_{out}(i)} f^k_{ac,ij} = 0 \quad \forall i,k \in \mathcal{N}_{\mathcal{NS}} \quad \forall k \neq i \tag{20}$$

$$\sum_{\mathcal{L}_{in}(i)} f^k_{dc,ij} - \sum_{\mathcal{L}_{out}(i)} f^k_{dc,ij} = 0 \quad \forall i,k \in \mathcal{N}_{\mathcal{NS}} \quad \forall k \neq i \tag{21}$$

$$-\epsilon_{ij} \leq f^k_{ac,ij} \leq \epsilon_{ij} \qquad \forall ij \in \mathcal{L} \tag{22}$$

$$-\lambda_{ij} \leq f^k_{dc,ij} \leq \lambda_{ij} \qquad \forall ij \in \mathcal{L} \tag{23}$$

$$\gamma_{ij} + \delta_{ij} - 1 \leq \epsilon_{ij} \qquad \forall ij \in \mathcal{L} \tag{24}$$

$$\gamma_{ij} - \delta_{ij} \leq \lambda_{ij} \qquad \forall ij \in \mathcal{L} \tag{25}$$

$$\sum_{\mathcal{L}} \gamma_{ij} \geq |\mathcal{N}| - |\mathcal{N}_S| \tag{26}$$

- Connection of AC lines to the HV/MV substation constraints

The constraints presented in (14)–(25) force AC and DC sub-grids to be forests. Thus, multiple AC sub-grids connected to the transmission only through converters could be an optimal solution considering only losses and converter costs. Nonetheless, this type of hybrid distribution grids can be difficult to operate from a control and protection perspective. Indeed, such an architecture would impact frequency stability in part of the network requiring a grid-forming control for the VSCs. With regard to protection, more circuit breakers would be required to protect each AC microgrid individually, resulting in an expensive protection scheme for the whole AC sub-grid.

To avoid this topology, it is necessary to require that the DC grid is downstream of the AC grid. In this case, it is equivalent to impose connectivity for the AC sub-grid and also impose at least one AC closed line connected to the HV/MV AC substation. Since the AC sub-grid is radial, this is the same as imposing a tree topology for the AC sub-grid. This is done by adding the supplementary variable θ_{ij}, representing AC closed lines state, and corresponding tree constraints in (27)–(29), which are based on Theorem 1.

$$\gamma_{ij} + \delta_{ij} - 1 \leq \theta_{ij} \leq \frac{\gamma_{ij} + \delta_{ij}}{2} \qquad \forall ij \in \mathcal{L} \tag{27}$$

$$\sum_{\mathcal{L}} \theta_{ij} = \sum_{\mathcal{N}} (\alpha_i) - |\mathcal{N}_S| \tag{28}$$

$$\sum_{\mathcal{L}(i)} \theta_{ij} \geq 1 \quad \forall i \in \mathcal{N}_{\mathcal{S}} \tag{29}$$

Theorem 1: A graph of order $|\mathcal{N}|$ is a tree if and only if it is acyclic and contains $|\mathcal{N}| - |\mathcal{N}_S|$ edges [26] (30)–(39) shown at the top of the next page.

The constraint for connection between DC sub-grids is less useful than the AC case, because multiple DC disconnected sub-grids are much easier to operate than multiple AC sub-grids. Moreover, the implementation of different DC links in an AC grid can be advantageous to balance distribution feeders loading and reduce losses [2]. Nevertheless, in the case where there is a HV/MV DC substation node, DC tree restriction can be useful to impose the connection of DC sub-grids to this node and improve voltage stability. Its formulation would follow same principle as for AC tree constraint with an additional variable for DC closed line state and related constraints.

C. Power Flow Constraints

Besides topological constraints, power flow constraints must be also considered in the DSP. Eqs. (30)–(35) and (36)–(39) present respectively AC and DC power flow constraints using SOCP relaxation of Branch Flow Model, also known as DistFlow formulation [12]. The interface between AC and DC networks is made by the VSC equations detailed in (40)–(44). All the restrictions were adapted to extend the formulation to consider logic constraints through binary variables and Big-M method [12].

- AC PF constraints

(30)–(35) represent the AC power flow formulation. Eqs. (30)–(31) set active and reactive power injection at the nodes for each scenario. Note DC resources power is supposed to be injected in AC grid through local converters unless the node is DC ($\beta_i = 1$). Additionally, generators are required to provide optimal reactive power support. Eqs. (32)–(33) ensure balance between active and reactive power injection and flow through lines. Eqs. (34) represents voltage drop equation with a modification to consider if nodes are separated by either a DC or an open line. For instance, the constraint becomes an equality only if the line is simultaneously AC and closed. (35) concludes AC power flow formulation with a SOCP relaxation of apparent power equation. This constraint relaxes original equation to convert the problem into a convex formulation. Therefore, the exactness is guaranteed only if this constraint is binding, i.e. if the constraint holds with equality at the optimal point.

- DC PF constraints

In the same way as AC power flow constraints, (36)–(39) represent the DC power flow constraints. Eqs. (36)–(37) respectively set active power injection of DC resources and ensure balance between injection at the nodes and flow through lines in

$$P^s_{ac,i} = P^s_{g,ac,i} - P^s_{d,ac,i} + (1-\beta_i)(P^s_{g,dc,i} - P^s_{d,dc,i}) \quad \forall i \in \mathcal{N}_{\mathcal{NS}}\ \forall s \in \mathcal{S} \tag{30}$$

$$Q^s_{ac,i} = Q^s_{g,ac,i} - Q^s_{d,ac,i} \quad \forall i \in \mathcal{N}_{\mathcal{NS}}\ \forall s \in \mathcal{S} \tag{31}$$

$$\sum_{\mathcal{L}_{in}(i)} (p^s_{ac,ij} - r_{ac,ij} l^s_{ac,ij}) - \sum_{\mathcal{L}_{out}(i)} (p^s_{ac,ij}) + P^s_{ac,i} + P^s_{vsc,ac,i} = 0 \quad \forall i \in \mathcal{N} \quad \forall s \in \mathcal{S} \tag{32}$$

$$\sum_{\mathcal{L}_{in}(i)} (q^s_{ac,ij} - x_{ac,ij} l^s_{ac,ij}) - \sum_{\mathcal{L}_{out}(i)} (q^s_{ac,ij}) + Q^s_{ac,i} + Q^s_{vsc,ac,i} = 0 \quad \forall i \in \mathcal{N} \quad \forall s \in \mathcal{S} \tag{33}$$

$$-\overline{v_{ac}}(2-\delta_{ij}-\gamma_{ij}) \le v^s_{ac,i} - v^s_{j,ac} - 2(r_{ac,ij}p^s_{ac,ij} + x_{ac,ij}q^s_{ac,ij}) + (r^2_{ac,ij} + x^2_{ac,ij}) l^s_{ac,ij} \le \overline{v_{ac}}(2-\delta_{ij}-\gamma_{ij}) \quad \forall ij \in \mathcal{L} \quad \forall s \in \mathcal{S} \tag{34}$$

$$\sqrt{(2p^s_{ac,ij})^2 + (2q^s_{ac,ij})^2 + (l^s_{ac,ij} - v^s_{ac,i})^2} \le l^s_{ac,ij} + v^s_{ac,i} \quad \forall ij \in \mathcal{L} \quad \forall s \in \mathcal{S} \tag{35}$$

$$P^s_{dc,i} = \beta_i (P^s_{g,dc,i} - P^s_{d,dc,i}) \quad \forall i \in \mathcal{N} \quad \forall s \in \mathcal{S} \tag{36}$$

$$\sum_{\mathcal{L}_{in}(i)} (p^s_{dc,ij} - r_{dc,ij} l^s_{dc,ij}) - \sum_{\mathcal{L}_{out}(i)} (p^s_{dc,ij}) + P^s_{dc,i} + P^s_{vsc,dc,i} = 0 \quad \forall i \in \mathcal{N} \quad \forall s \in \mathcal{S} \tag{37}$$

$$-\overline{v_{dc}}(1+\delta_{ij}-\gamma_{ij}) \le v^s_{dc,i} - v^s_{j,dc} - 2r_{ij}p^s_{dc,ij} + r^2_{dc,ij} l^s_{dc,ij} \le \overline{v_{dc}}(1+\delta_{ij}-\gamma_{ij}) \quad \forall ij \in \mathcal{L}\ \forall s \in \mathcal{S} \tag{38}$$

$$\sqrt{(2p^s_{dc,ij})^2 + (l^s_{dc,ij} - v^s_{dc,i})^2} \le l^s_{dc,ij} + v^s_{dc,i} \quad \forall ij \in \mathcal{L} \quad \forall s \in \mathcal{S} \tag{39}$$

each node for each scenario. Eqs. (38) represents voltage drop equation decoupling nodes if they are separated by either an AC or open line. Eqs. (39) depicts a SOCP relaxation for power flow as a function of squared voltage and current.

- VSC constraints

VSCs can be modelled basically as AC and DC controllable voltage sources coupled through active power on each side and converter losses (see (40)). For planning purposes, these losses can be approximated by two terms respectively proportional to the rated power and to the apparent power of the converter (see (41)–(43)) [27]. This model is especially accurate for high loading operation of VSC, where efficiency is approximately constant for most advantageous topologies for MVDC applications [28]. Note that (43) is a SOCP relaxation, but exactness tends to be respected because losses in the system are minimized by objective function. The converter apparent power is limited by the SOCP constraint depicted in (44).

$$P^s_{vsc,i} + P^s_{vsc,dc,i} + P^s_{vsc,l,i} = 0 \quad \forall i \in \mathcal{N}\ \forall s \in \mathcal{S} \tag{40}$$

$$P^s_{vsc,l,i} = P^s_{vsc,l0,i} + P^s_{i,vsc,l1} \quad \forall i \in \mathcal{N} \quad \forall s \in \mathcal{S} \tag{41}$$

$$P^s_{vsc,l0,i} = c_0 S_{vsc,rated,i} \quad \forall i \in \mathcal{N} \quad \forall s \in \mathcal{S} \tag{42}$$

$$c_1 \sqrt{(P^s_{vsc,ac,i})^2 + (Q^s_{vsc,ac,i})^2} \le P^s_{vsc,l1,i} \quad \forall i \in \mathcal{N} \quad \forall s \in \mathcal{S} \tag{43}$$

$$\sqrt{(P^s_{vsc,ac,i})^2 + (Q^s_{vsc,ac,i})^2} \le S_{vsc,rated,i} \quad \forall i \in \mathcal{N} \quad \forall s \in \mathcal{S} \tag{44}$$

D. Operational Constraints

Additional constraints with regard to operational limits are also considered. All these constraints use binary variables to bind the continuous variables as a function of the choice between AC or DC for the nodes and lines as well as open or closed for the lines. Eqs. (45)–(46) impose AC and DC MV voltage limits. Eqs. (47)–(52) define boundaries respectively to AC active and reactive power and current setting both to zero if the line is DC or open. Analogously, (53)–(56) impose limits respectively to DC active power and current setting both to zero if the line is AC or open. Eqs. (57) limits rated power of VSC to a maximum and forces it to be zero if no system converter is installed at the node. Eqs. (58)–(59) respectively limit reactive power support of AC distributed generation and DC distributed generation local converter according to their capacities. Eq. (60) imposes that if there is a substation converter, there are no local AC/DC converters and no reactive power support corresponding to these resources is done.

$$\underline{v_{ac}}(\alpha_i + a_i - a_i\alpha_i) \le v^s_{ac,i} \le \overline{v_{ac}}(\alpha_i + a_i - a_i\alpha_i) \quad \forall i \in \mathcal{N} \quad \forall s \in \mathcal{S} \tag{45}$$

$$\underline{v_{dc}}\beta_i \le v^s_{dc,i} \le \overline{v_{dc}}\beta_i \quad \forall i \in \mathcal{N} \quad \forall s \in \mathcal{S} \tag{46}$$

$$0 \le l^s_{ac,ij} \le \overline{l_{ac,ij}}\delta_{ij} \quad \forall ij \in \mathcal{L} \quad \forall s \in \mathcal{S} \tag{47}$$

$$l^s_{ac,ij} \le \overline{l_{ac,ij}}\gamma_{ij} \quad \forall ij \in \mathcal{L} \quad \forall s \in \mathcal{S} \tag{48}$$

$$-\overline{p_{ac,ij}}\delta_{ij} \le p^s_{ac,ij} \le \overline{p_{ac,ij}}\delta_{ij} \quad \forall ij \in \mathcal{L} \quad \forall s \in \mathcal{S} \tag{49}$$

$$-\overline{q_{ac,ij}}\delta_{ij} \le q^s_{ac,ij} \le \overline{q_{ac,ij}}\delta_{ij} \quad \forall ij \in \mathcal{L} \quad \forall s \in \mathcal{S} \tag{50}$$

$$-\overline{p_{ac,ij}}\gamma_{ij} \le p^s_{ac,ij} \le \overline{p_{ac,ij}}\gamma_{ij} \quad \forall ij \in \mathcal{L} \quad \forall s \in \mathcal{S} \tag{51}$$

$$-\overline{q_{ac,ij}}\gamma_{ij} \le q^s_{ac,ij} \le \overline{q_{ac,ij}}\gamma_{ij} \quad \forall ij \in \mathcal{L} \quad \forall s \in \mathcal{S} \tag{52}$$

TABLE I
CASE STUDY PLANNING PARAMETERS.

Parameter	Value
Base values (S, V_{ac} and V_{dc})	10MVA, 4.16kV and 6.8kV
Voltage magnitude limits	$\pm 5\%$
c_0	0.0001 [28]
c_1	0.0177 [28]
Load growth	0.7%/year [8]
Discount rate	7.5% [8]
VSC service life in years	15 years [8]
VSC capital cost coefficient	170$/kVA [8]
VSC maintenance cost coefficient	5% of capital cost [8]
Losses cost	0.08$/kWh [19]

$$0 \leq l^s_{dc,ij} \leq \overline{l_{dc,ij}}(1-\delta_{ij}) \quad \forall ij \in \mathcal{L} \quad \forall s \in \mathcal{S} \tag{53}$$

$$l^s_{dc,ij} \leq \overline{l_{dc,ij}}\gamma_{ij} \quad \forall ij \in \mathcal{L} \quad \forall s \in \mathcal{S} \tag{54}$$

$$-\overline{p_{dc,ij}}(1-\delta_{ij}) \leq p^s_{dc,ij} \leq \overline{p_{dc,ij}}(1-\delta_{ij}) \quad \forall ij \in \mathcal{L} \quad \forall s \in \mathcal{S} \tag{55}$$

$$-\overline{p_{dc,ij}}\gamma_{ij} \leq p^s_{dc,ij} \leq \overline{p_{dc,ij}}\gamma_{ij} \quad \forall ij \in \mathcal{L} \quad \forall s \in \mathcal{S} \tag{56}$$

$$0 \leq S_{vsc,rated,i} \leq \overline{S_{vsc}}\zeta_i \quad \forall i \in \mathcal{N} \quad \forall s \in \mathcal{S} \tag{57}$$

$$\sqrt{(P^s_{g,ac,i})^2 + (Q^s_{g,ac,i})^2} \leq \overline{S_{g,ac}} \quad \forall i \in \mathcal{N} \quad \forall s \in \mathcal{S} \tag{58}$$

$$\sqrt{(P^s_{g,dc,i})^2 + (Q^s_{g,dc,i})^2} \leq \overline{S_{g,dc}} \quad \forall i \in \mathcal{N} \quad \forall s \in \mathcal{S} \tag{59}$$

$$-\overline{S_{g,dc}}(1-\zeta_i) \leq Q^s_{g,dc,i} \leq \overline{S_{g,dc}}(1-\zeta_i) \quad \forall i \in \mathcal{N} \quad \forall s \in \mathcal{S} \tag{60}$$

IV. RESULTS

The goal of this planning is to determine the most economical topology of a distribution system considering that the DSO intends to expand an existing network to accomodate DC distributed resources. To evaluate the presented AC/DC DSP model, a case study of a distribution system with high penetration of DER and close to its operational limits was considered.

The proposed formulation was implemented in the YALMIP optimization toolbox [29] with MATLAB R2020b, solved by Gurobi [30], on a laptop equipped with a 1.70 GHz Intel Core™ i5-10310 U CPU and 16 GB RAM. The MIP optimality gap was set to 1% [12].

A. Case Study

In this work, a case study based on an AC distribution system proposed by [8] is considered. All the voltage limits, type of DC system and capacity, length and impedance of the lines are the same as in the original study. The grid is connected to the transmission system and it consists of several DER: photo-voltaic power plants (PV), a wind turbine (WT), a diesel generator set (DGS) and electrical vehicle charging stations (EV). Moreover, AC and DC loads are also connected to this grid. The details of planning parameters, generation and load data are respectively presented in Tables I, II, and III.

TABLE II
DISTRIBUTION SYSTEM GENERATION DATA [8]

Bus	DG Type	$\overline{P_{g,ac}}$ (MW)	$\overline{P_{g,dc}}$ (MW)
4	PV	-	1.50
7	PV	-	1.50
9	WT	-	1.00
11	PV	-	1.50
13	DGS	2.00	-

TABLE III
DISTRIBUTION SYSTEM LOAD DATA.

Bus	$P_{d,ac}$ (MW)	$Q_{d,ac}$ (MVAr)	$P_{d,dc}$ (MW)
1	-	-	-
2	0.65	0.29	-
3	-	-	1.25
4	0.33	0.16	-
5	0.33	0.16	0.32
6	0.49	0.23	0.49
7	0.33	0.16	-
8	0.33	0.16	1.25
9	-	-	0.65
10	0.33	0.16	0.33
11	-	-	-
12	-	-	1.25
13	0.49	0.22	-

TABLE IV
REPRESENTATIVE SCENARIOS USED IN THE DSP.

		Modulation coefficient		
		Low	Medium	High
LD	m^s_{LD}	0.53	0.75	0.94
	w^s_{LD}	0.34	0.25	0.41
PV	m^s_{PV}	0.06	0.31	0.75
	w^s_{PV}	0.65	0.20	0.15
WT	m^s_{WT}	0.20	0.39	0.89
	w^s_{WT}	0.40	0.36	0.24
EV	m^s_{EV}	0.10	0.45	0.80
	w^s_{EV}	0.33	0.26	0.41

Because [8] allowed constraints violation in 5% of the scenarios and also authorized meshed topology, the maximum load was reduced by 35% to avoid infeasible scenarios for AC planning in this article. Note that the wind turbine power plant was considered as a DC source in this case because even though this resource is typically embedded with AC generators, most of variable speed wind turbine require a DC conversion stage to be connected to the grid because of frequency mismatch.

The load demand (LD), PV, WT and EV active power are modeled as stochastic parameters. Therefore, the maximum power of each resource is modulated by a coefficient (m^s_{LD}, m^s_{PV}, m^s_{WT} and m^s_{EV}) for each scenario as represented in (61). These modulation coefficients are respectively linked to a weigh factor w^s which can be obtained with (62) and parameters shown in Table IV, satisfying (63).

$$P^s_{\diamond} = m^s_{\diamond} \times \overline{P^s_{\diamond}} \quad \forall \diamond \in \{LD, PV, WT, EV\} \forall s \in \mathcal{S} \tag{61}$$

$$w^s = w^s_{LD} \times w^s_{PV} \times w^s_{WT} \times w^s_{EV} \quad \forall s \in \mathcal{S} \tag{62}$$

$$\sum_{\mathcal{S}} w^s = 1 \tag{63}$$

[8] generated a large number of random scenarios through the empirical cumulative distribution function of stochastic parameters for each season and performed Monte Carlo simulations to carry DSP. Here, a scenario reduction methodology based on minimizing the Wasserstein distance was applied (see [19]) to effectively capture the inherent uncertainty of stochastic resources. The approach used involves generating a limited number of representative scenarios that are derived from the distribution function coefficients previously established in [8]. 3 scenarios (low, medium and high modulation coefficient) were considered to represent the probability distribution function of each one of the 4 stochastic resources. In addition, load growth was modeled through time stages to represent accumulated effect in the maximum demand, as it is often done in expansion planning such as in [31]. To avoid computational burden associated to a large number of scenarios, it has been decided to consider 2 time stages with steps in demand in the beginning and in the middle of planning time, making 6 scenarios for load demand in total. This choice is done by the DSO and depends on the studied area and relevant public information on load expansion. Then, under the hypothesis that resources availability and load demand are independent [32], scenarios were combined to generate $6 \times 3 \times 3 \times 3 = 162$ representative scenarios.

In order to assess the robustness of the topology optimization, two critical scenarios were simulated. The first scenario considered the maximum load demand and EV load without any generation. The second scenario considered maximum generation from WT and PV with minimum load and EV. Through these simulations, the worst-case scenario was evaluated to ensure the system's operation under worst-case scenarios.

Other changes are also considered in comparison to the original case study. First, the network is required to be operated radially. DGs are also required to optimally support the network with reactive power respecting the power capacity limits of the converter when connected to an AC bus. With respect to planning parameters, load growth, discount rate and VSC cost and service life are the same as in the original case study [8]. Finally, the planning performed in this study is from a DSO standpoint addressing the modification of an existing power system, where DC DER owners can be required to be connected to a DC system. Accordingly, neither DER installation and generation cost nor cable cost are considered and only VSCs used to form the MVDC network are considered in DSO costs.

B. Planning Results

To study the benefits of AC/DC topology, simulations were performed to obtain AC and AC/DC planning. For the first planning, δ was set to one to impose that all the lines are AC. From other basic topological constraints, it follows that no VSC is installed and the optimization becomes an AC reconfiguration problem with reactive power support of DGs (PV and WT) and voltage control in HV/MV AC substation through transformer on-load tap changer. The result of AC planning is depicted in Fig. 5(a).

The AC/DC optimal topology obtained is shown in Fig. 5(b). This topology requires a new network configuration and the

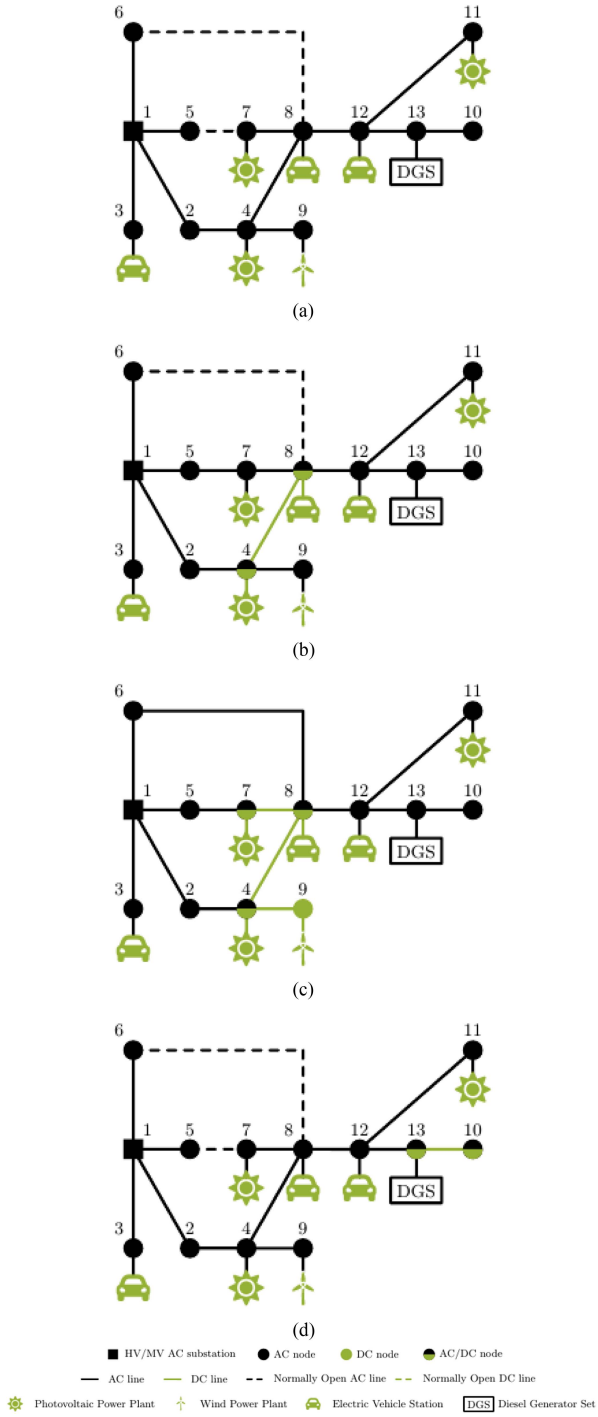

Fig. 5. Optimal topology planning of case study: (a) AC DSP, (b) AC/DC DSP, (c) AC/DC losses minimization with meshed topology but piecewise radial and (d) AC/DC losses minimization losses with full radial topology.

conversion of the line connecting nodes 4 and 8 into a DC. Losses are hence reduced in the operation of the grid by 33% through active power transfer and conversion of one line into DC using the system converters installed. Node 4 and 8 also present a significant penetration of DC resources (DC load, PV and EV), which are now supplied by the DC side of the system's converter. All these effects lead the system to a reduction of approximately 20% in Net Present Value of the total costs (see

TABLE V
DSO EXPENDITURES OF AC AND AC/DC DSP.

	Net Present Value (M$)	CAPEX (M$)	OPEX Present Value (M$)
AC DSP	1.968	0	1.968
AC/DC DSP	1.562	0.167	1.395

TABLE VI
AVERAGE LOSSES IN THE DISTRIBUTION SYSTEM.

	Average losses (kW)			Total losses/ Total generation
	AC lines	DC lines	VSC	
AC DSP	642	-	-	13.2%
AC/DC DSP	383	23	22	7.5%
AC/DC losses minimization meshed	231	32	32	5.0%
AC/DC losses minimization radial	311	6	24	5.9%

Table V), confirming the interest of an AC/DC architecture for the studied distribution system.

Furthermore, the distribution system is no longer radial, because line connecting nodes 5 and 7 is henceforth closed. Nonetheless, AC and DC sub-grids are radial and a simple protection strategy can be employed. This shows the benefits of using topological constraints for piecewise radiality instead of enforcing radiality for the whole grid. This meshed but piecewise radial AC/DC topology can also improve network reliability against component failures, i.e. N-1 criterion [33].

It is important to note that only one line was converted into DC at the optimal solution in the case study considered. This happens because local converters costs are not considered in DSO total expenditures. Thus, investing in system converters to have DC lines and reduce losses over the network is less advantageous than to demand DC resources holders to connect to AC nodes through local converters. This result is actually more aligned with reality at MV level, where AC/DC distribution networks are rather in demonstration stage (see [34] and [35]) and appear to be an optimal solution in the planning of new networks from scratch, but not necessarily in expansion planning under a unbundling regulation.

Losses minimization was also tested as objective function (see (7)) to analyze the full capability to increase efficiency of a hybrid distribution grid despite of economic aspects and to compare proposed topological constraints with existing literature. The optimization with meshed but piecewise radial topology results in a higher presence of DC lines, forming a DC grid in the area of high penetration of DC DER (see Fig. 5(c)).

In opposition, optimal AC/DC full radial topology commonly found in the literature only has one DC line, as presented in Fig. 5(d). This line enabled the reduction of losses in a line with high power flow due to the presence of a DGS in node 13 and both AC and DC loads in node 10. The AC/DC grid architecture with topological constraints led to an average reduction of losses of 55% and 17% losses in comparison to full AC planning and full radial AC/DC losses minimization respectively, as depicted Table VI. Thus, it is clear that incorporating proposed constraints can lead to efficient hybrid architectures for distribution grids, emphasizing the importance of including them in the modeling process.

TABLE VII
MODIFIED IEEE 33 BUS DISTRIBUTION SYSTEM GENERATION DATA.

Bus	DG Type	$\overline{P_{g,dc}}$ (MW)
8	PV	0.50
21	PV	0.50
25	PV	0.50
28	PV	0.50
30	PV	0.50

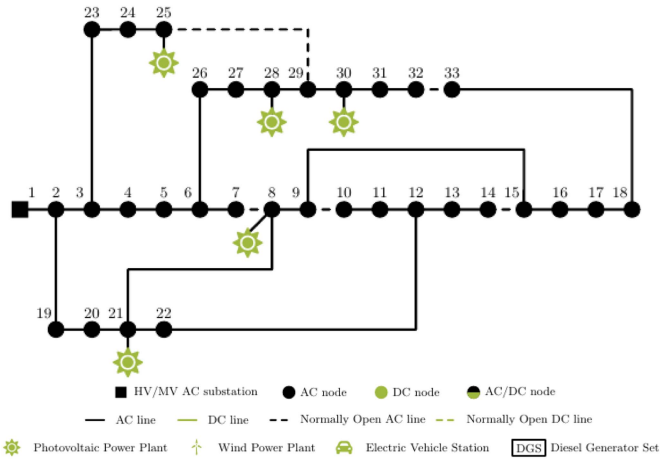

Fig. 6. Optimal topology of modified IEEE 33 bus distribution system case study.

TABLE VIII
COMPUTATION TIME OF OPTIMAL DSP.

Case	Model	Number of Lines	Number of Scenarios	Computation Time
13 bus	AC DSP	14	162	$0h03$
	AC/DC DSP	14	162	$9h21$
IEEE 33 bus	AC DSP	37	18	$0h03$
	AC/DC DSP	37	18	$5h08$

C. Computational Efficiency

To study computation performance of proposed model, another case study based on modified IEEE 33 bus distribution system [6] was simulated. Only PV connection was considered in the network according to Table VII. Same planning parameters and uncertainty modelling as previous case study were adopted. Therefore, 3 scenarios for PV uncertainty and 6 scenarios for LD uncertainty and load growth were considered, resulting 18 scenarios. Both AC and AC/DC DSP optimization result in a full AC topology as shown in Fig. 6. As previously discussed, this occurs because, from an economic point of view of DSO, converting part of a system into DC may not be as beneficial if the network losses are relatively low in AC operation.

Regardless, the present findings offer means to evaluate the running time of AC and AC/DC DSP models for a larger system, as presented in Table VIII. In the AC/DC case, the considerable number of topologies generating feasible solutions contributes to a much longer computation time. As such, the utilization of

TABLE IX
EXACTNESS OF AC/DC DSP.

Case	Model	gap_{ac}	gap_{dc}	gap_{vsc}
13 bus	AC DSP	8.8×10^{-8}	-	-
	AC/DC DSP	4.7×10^{-8}	7.4×10^{-9}	1.2×10^{-7}
IEEE 33 bus	AC DSP	4.4×10^{-5}	-	-
	AC/DC DSP	2.1×10^{-7}	-	-

clustering techniques may be required to solve AC/DC DSP with topological constraints for larger networks by dividing them into smaller grids. An alternative approach to decrease running time is to enhance scenario reduction methods to obtain fewer representative scenarios without compromising information about resources uncertainty.

Moreover, it is also important to note that MISOCP models privilege accuracy and optimality over running time. Indeed, the computation time obtained has been reported in the literature for similar methods [11] and is justifiable as long-term planning studies are typically conducted for decision-making purposes on a multi-year timescale.

With respect to model accuracy, the exactness of SOCP relaxations used in the modelling of AC (35), DC (39) and VSC ((43)) can be evaluated respectively through the computation of the gap for each line/VSC according to (64)–(66). The gap is a metric representing the relaxation error, i.e. it indicates how close the relaxed constraints are to be satisfied as an equality at the optimal solution. It is not computed whenever the denominator of its expression is zero.

$$gap_{ac} = \max\left(\frac{l^s_{ac,ij} + v^s_{ac,i}}{\sqrt{(2p^s_{ac,ij})^2 + (2q^s_{ac,ij})^2 + (l^s_{ac,ij} - v^s_{ac,i})^2}} - 1\right) \tag{64}$$

$$gap_{dc} = \max\left(\frac{l^s_{dc,ij} + v^s_{dc,i}}{\sqrt{(2p^s_{dc,ij})^2 + (l^s_{dc,ij} - v^s_{dc,i})^2}} - 1\right) \tag{65}$$

$$gap_{vsc} = \max\left(\frac{P^s_{vsc,l1,i}}{c_1\sqrt{(P^s_{vsc,ac,i})^2 + (Q^s_{vsc,ac,i})^2}} - 1\right) \tag{66}$$

The gap obtained for each equation for each case study is very small (see Table IX), indicating a nearly exact relaxation.

D. Discussions on Market Regulation

The performed numeric studies show that AC/DC converter ownership aspects are relevant in hybrid expansion planning under unbundled electricity market regulation. In this context, since the DSO is responsible for topological planning, its perspective needs to be considered. Indeed, converters costs can shift from DER holders to the DSO in hybrid topology, jeopardizing AC/DC planning economic viability. Furthermore, the results indicate that the advantages of hybrid AC/DC topology is restricted to cases where the system operates close to its operational limits, as in real-life case study studied in [35]. Therefore, expansion planning costs sharing between DER holders and DSO needs to be further investigated to better assess the interest of AC/DC topology. In future work, market regulation design can be addressed to study the impact of market structure on the MV optimal topological choice.

V. CONCLUSION

In this article, a novel formulation for hybrid AC/DC planning of distribution system is proposed. The model developed considers topological constraints to guarantee that AC and DC sub-grids are radial. The connectivity of AC grid to the HV/MV substation is also implemented in the optimization problem formulation. A realistic and innovative approach from DSO perspective is adopted for the case study, considering the modification of an existing distribution system and converters ownership issues to model unbundled market regulation impact on optimal topology. The effectiveness of the proposed model specially for overloaded systems is demonstrated by decreasing total costs through reduction of losses in the case study.

Moreover, the exactness of the relaxation is verified and global optimality is guaranteed by the solver used. The results indicate the interest of topological constraints, showing that grids with hybrid loops are potentially a good compromise between flexibility in the power flow and protection simplicity. The formulation also allows an easy inclusion of other customized topological constraints, such as imposing certain lines or nodes to be AC or DC for specific reasons. In summary, the developed model provides a systematic tool for long-term planning studies for DSOs to optimally identify economic target architectures for existing distribution grids.

In future work, scenario generation can be improved to reduce the number of scenarios while keeping information about the stochastic parameters and clustering methods to divide large distribution systems in small ones to solve the problem could improve computational performance. Additionally, N-1 criterion analysis may be considered to assess AC/DC distribution topology from a reliability point-of-view. Finally, market regulation and planning costs sharing can be investigated to better assess the potential value of AC/DC hybrid topology.

REFERENCES

[1] M. Monadi, K. Rouzbehi, J. Ignacio Candela, and P. Rodriguez, "DC distribution networks: A solution for integration of distributed generation systems," in *Distributed Generation Systems*, G. B. Gharehpetian, S. Mohammad, and M. Agah, eds. Oxford, U.K.: Butterworth-Heinemann, 2017, Ch. 11, pp. 509–561.

[2] L. Zhang, J. Liang, W. Tang, G. Li, Y. Cai, and W. Sheng, "Converting AC distribution lines to DC to increase transfer capacities and DG penetration," *IEEE Trans. Smart Grid*, vol. 10, no. 2, pp. 1477–1487, Mar. 2019.

[3] X. Liu, Y. Liu, Y. Xiang, and X. Yuan, "Optimal planning of AC-DC hybrid transmission and distributed energy resource system: Review and prospects," *CSEE J. Power Energy Syst.*, vol. 5, no. 3, pp. 409–422, Sep. 2019.

[4] G. Li, L. Zhang, T. Joseph, J. Liang, and G. Yan, "Comparisons of MVAC and MVDC systems in dynamic operation, fault protection and post-fault restoration," in *Proc. IEEE 45th Annu. Conf. Ind. Electron. Soc.*, 2019, pp. 5657–5662.

[5] Y. Fan et al., "Key technologies for medium and low voltage DC distribution system," *Glob. Energy Interconnection*, vol. 4, no. 1, pp. 91–103, Feb. 2021.

[6] Y. Yang et al., "Multi-objective coordinated planning of distributed generation and AC/DC hybrid distribution networks based on a multi-scenario technique considering timing characteristics," *Energies*, vol. 10, no. 12, Dec. 2017, Art. no. 2137.
[7] A. Ghadiri, Mahmoud R. Haghifam, and S. M. M. Larimi, "Comprehensive approach for hybrid AC/DC distribution network planning using genetic algorithm," *IET Gener. Transmiss. Distrib.*, vol. 11, no. 16, pp. 3892–3902, Nov. 2017.
[8] H. M. A. Ahmed, A. B. Eltantawy, and M. M. A. Salama, "A planning approach for the network configuration of AC–DC hybrid distribution systems," *IEEE Trans. Smart Grid*, vol. 9, no. 3, pp. 2203–2213, May 2018.
[9] Z. Sabzian-Molaee, E. Rokrok, and M. Doostizadeh, "An optimal planning model for AC-DC distribution systems considering the converter lifetime," *Int. J. Elect. Power Energy Syst.*, vol. 138, Jun. 2022, Art. no. 107911.
[10] H. M. A. Ahmed, A. B. Eltantawy, and M. M. A. Salama, "A reliability-based stochastic planning framework for AC–DC hybrid smart distribution systems," *Int. J. Elect. Power Energy Syst.*, vol. 107, pp. 10–18, May 2019.
[11] X. Wu, Z. Wang, T. Ding, and Z. Li, "Hybrid AC/DC microgrid planning with optimal placement of DC feeders," *Energies*, vol. 12, no. 9, May 2019, Art. no. 1751.
[12] Z. Wu, P. Liu, W. Gu, H. Huang, and J. Han, "A bi-level planning approach for hybrid AC–DC distribution system considering N-1 security criterion," *Appl. Energy*, vol. 230, pp. 417–428, Nov. 2018.
[13] Z. Wu, Q. Sun, W. Gu, Y. Chen, H. Xu, and J. Zhang, "AC/DC hybrid distribution system expansion planning under long-term uncertainty considering flexible investment," *IEEE Access*, vol. 8, pp. 94956–94967, 2020.
[14] D. K. Molzahn and I. A. Hiskens, "A survey of relaxations and approximations of the power flow equations," *Foundations Trends Electric Energy Syst.*, vol. 4, no. 1/2, pp. 1–221, 2019.
[15] M. Baradar, M. R. Hesamzadeh, and M. Ghandhari, "Second-order cone programming for optimal power flow in VSC-Type AC–DC grids," *IEEE Trans. Power Syst.*, vol. 28, no. 4, pp. 4282–4291, Nov. 2013.
[16] S. Bahrami, F. Therrien, V. W. S. Wong, and J. Jatskevich, "Semidefinite relaxation of optimal power flow for AC–DC grids," *IEEE Trans. Power Syst.*, vol. 32, no. 1, pp. 289–304, Jan. 2017.
[17] H. Ergun, J. Dave, D. Van Hertem, and F. Geth, "Optimal power flow for AC–DC grids: Formulation, convex relaxation, linear approximation, and implementation," *IEEE Trans. Power Syst.*, vol. 34, no. 4, pp. 2980–2990, Jul. 2019.
[18] S. Mohamed, M. F. Shaaban, M. Ismail, E. Serpedin, and K. A. Qaraqe, "An efficient planning algorithm for hybrid remote microgrids," *IEEE Trans. Sustain. Energy*, vol. 10, no. 1, pp. 257–267, Jan. 2019.
[19] C. Wang, G. Song, P. Li, H. Ji, J. Zhao, and J. Wu, "Optimal siting and sizing of soft open points in active electrical distribution networks," *Appl. Energy*, vol. 189, pp. 301–309, Mar. 2017.
[20] "Directive (EU) 2019/944 of the European Parliament and of the Council on common rules for the internal market for electricity and amending Directive 2012/27/EU," ch. 4., 2019. [Online]. Available: https://eur-lex.europa.eu/legal-content/EN/TXT/?uri=celex%253A32019L0944
[21] Y. Huang, K. Alvehag, and L. Soder, "Regulation impact on distribution systems with distributed generation," in *Proc. IEEE 9th Int. Conf. Eur. Energy Market*, 2012, pp. 1–8.
[22] H. Ahmadi and J. R. Martí, "Mathematical representation of radiality constraint in distribution system reconfiguration problem," *Int. J. Elect. Power Energy Syst.*, vol. 64, pp. 293–299, Jan. 2015.
[23] M. Lavorato, J. F. Franco, M. J. Rider, and R. Romero, "Imposing radiality constraints in distribution system optimization problems," *IEEE Trans. Power Syst.*, vol. 27, no. 1, pp. 172–180, Feb. 2012.
[24] M. K. Singh, V. Kekatos, S. Taheri, K. P. Schneider, and C.-C. Liu, "Enforcing radiality constraints for DER-aided power distribution grid reconfiguration," 2019, *arXiv:1910.03020*.
[25] S. Lei, C. Chen, Y. Song, and Y. Hou, "Radiality constraints for resilient reconfiguration of distribution systems: Formulation and application to microgrid formation," *IEEE Trans. Smart Grid*, vol. 11, no. 5, pp. 3944–3956, Sep. 2020.
[26] J. Harris, Jeffry L. Hirst, and M. Mossinghoff, "Combinatorics and graph theory," in *Undergraduate Texts in Mathematics*. New York, NY, USA: Springer, 2008.
[27] H. Ji, C. Wang, P. Li, F. Ding, and J. Wu, "Robust operation of soft open points in active distribution networks with high penetration of photovoltaic integration," *IEEE Trans. Sustain. Energy*, vol. 10, no. 1, pp. 280–289, Jan. 2019.
[28] G. Abeynayake, G. Li, T. Joseph, J. Liang, and W. Ming, "Reliability and cost-oriented analysis, comparison and selection of multi-level MVdc converters," *IEEE Trans. Power Del.*, vol. 36, no. 6, pp. 3945–3955, Dec. 2021.
[29] J. Lofberg, "YALMIP: A toolbox for modeling and optimization in MATLAB," in *Proc. IEEE Int. Conf. Robot. Automat.*, 2004, pp. 284–289.
[30] Gurobi Optimization, LLC. Gurobi Optimizer Reference Manual, 2022. [Online]. Available: https://www.gurobi.com
[31] H. Falaghi, C. Singh, M.-R. Haghifam, and M. Ramezani, "DG integrated multistage distribution system expansion planning," *Int. J. Elect. Power Energy Syst.*, vol. 33, no. 8, pp. 1489–1497, Oct. 2011.
[32] A. Garry, M.-C. Alvarez-Herault, F. Cadoux, and N. Hadjsaid, "Probabilistic modelling of renewable generation to account for uncertainties in interconnection studies," *Int. Trans. Elect. Energy Syst.*, vol. 29 no. 10, Oct. 2019, Art. no. e12091.
[33] L. Wu, B. Geng, H. Liu, Z. Piao, H. Wang, and Z. Lin, "Reliability assessment of AC/DC hybrid distribution network based on sequential monte carlo method," in *Proc. IEEE 5th Asia Conf. Power Elect. Eng.*, 2020, pp. 1096–1100.
[34] W. Li et al., "State of the art of researches and applications of MVDC distribution systems in power grid," in *Proc. IEEE 45th Annu. Conf. Ind. Electron. Soc.*, 2019, pp. 5680–5685.
[35] J. Yu, K. Smith, M. Urizarbarrena, N. MacLeod, R. Bryans, and A. Moon, "Initial designs for the ANGLE DC project; converting existing AC cable and overhead line into DC operation," in *Proc. 13th IET Int. Conf. AC DC Power Transmiss.*, 2017, pp. 1–6.

Heitor Farias de Barros (Student Member, IEEE) received the M.S. degree in electrical engineering from the Grenoble INP, Grenoble, France, in 2020. He is currently working toward the Ph.D. degree in electric engineering with G2Elab - Grenoble INP. His general research interests include planning, reliability, protection and control of hybrid distribution systems.

Marie-Cécile Alvarez-Herault (Member, IEEE) received the M.S. and Ph.D. degrees in electrical engineering from the Grenoble INP, Grenoble, France, in 2007 and 2009. Since 2010, she has been an Associate Professor with the University Grenoble Alpes, Grenoble, and the main French DSO, Enedis, Smart grids industrial chair holder since 2021. Her main research interests include distribution network planning and in particular the investment decisions under uncertainties.

Bertrand Raison (Senior Member, IEEE) received the M.S. and Ph.D. degrees in electrical engineering from the Grenoble INP, Grenoble, France, in 1996 and 2000, respectively. Since 2009, he has joined the Université Grenoble Alpes - G2Elab as a Professor. His general research interests include protection, fault detection, and localization in electrical systems.

Quoc Tuan Tran (Senior Member, IEEE) received the Ph.D. degree in electrical engineering from the Grenoble INP, Grenoble, France, in 1993. He is currently a Professor with INSTN - Paris Saclay University, Paris, France, and a Scientific Manager with Alternative Energies and Atomic Energy Commission (CEA-INES). His research interests include power system analysis, operations, electromagnetic transients, distributed generation, smart-grid and renewable energy